Extended Abstracts of the 1996 International Conference on Solid State Devices and Materials, Yokohama, 1996, pp. 862-863

Octahedral Void Structure Observed at the Grown-In Defects in the Bulk of Standard CZ-Si for MOSLSIs

Takemi Ueki, Manabu Itsumi and Tadao Takeda
LSI Laboratories, NTT, Atsugi-Shi, Kanagawa Pref., 243-01 Japan

Gate oxide defects are a major factor influencing the yield and reliability of MOSLSIs. The defect density of oxides thermally grown on Czochralski silicon (CZ-Si) is clearly larger than that of oxides thermally grown on float-zone silicon (FZ-Si), as shown in Fig. 1. The origin of the oxide defects may be the grown-in defects (micro defects) in CZ-Si. In recent studies, copper decoration followed by FIB thinning of samples revealed an octahedral void structure just beneath the oxide defects [1-2]. This observation is based on the copper decoration, which might have some influence on the defect structure. In this study, we tried to observe the grown-in defect directly, without the influence of copper decoration.

The wafers used were 6-inch-diameter (100)-oriented standard CZ-Si wafers. The sample preparation procedure is shown in Fig. 2. First, the wafers were cleaved to form samples. Three-dimensional coordinates of grown-in defects were measured with IR-tomography. The samples were thinned by FIB to about 0.3 um for TEM observation. Then they were analyzed with energy-dispersive X-ray spectroscopy (EDS). Analysis by Auger electron spectroscopy (AES) with a more precise detection limit was also made with Ar sputtering.

A typical example of the grown-in defects is shown in a cross-sectional TEM image in Fig. 3(a). The defects are twin type, octahedral defects about 100 nm in size. The face of the side walls was identified as <111> plane. These features were common for five TEM images that were obtained. Magnification of the image revealed the existence of a 2-nm-thick layer on the side walls (Fig. 3(b)). The thin layer completely covers the side walls uniformly. EDS spectra (for Points A and B in Fig. 3) showed that Si was detected but oxygen was not detected (Fig. 4). If the octahedron defect is filled with SiO_2, oxygen signals can be detected. In addition, the intensity of the Si signal for the defect (Point A) is clearly smaller than that of Si signal for the Si matrix (Point B), which suggests that the octahedron defect is void. AES results revealed that the intensity of the Si signal for the defect (Point A) is clearly smaller than that of Si signal for the Si matrix (Point B), which agrees with the results of EDS (Fig. 5). Moreover, AES results revealed that the intensity of the oxygen signal for the defect (Point A) is a little larger than that of the oxygen signal for the Si matrix (Point B), suggesting that the 2-nm-thick layer on the side wall is SiO_2.

The above results show that the octahedral void structure is formed during Si-ingot growth. Agglomeration of vacancies during the Si-ingot growth may result in the formation of the void. The 2-nm-thick layer may be formed at the final stage of the formation of the octahedral void structure during the Si-ingot growth. Diffusion and agglomeration of vacancies during the Si-ingot growth should be further investigated by both experiment and simulation.

To summarize, we clarified that the octahedral void structure with a 2-nm-thick layer was formed during CZ-Si crystal growth. Agglomeration of vacancies during the Si-ingot growth may be closely related to the formation of the void. Our analysis suggests that the 2-nm-thick layer is SiO_2.

[1] M. Itsumi et al., J. Appl. Phys., 78(10), 5984 (1995).
[2] M. Itsumi et al., Jpn. J. Appl. Phys., Vol. 35, No. 1, No. 2B, 812 (1996).

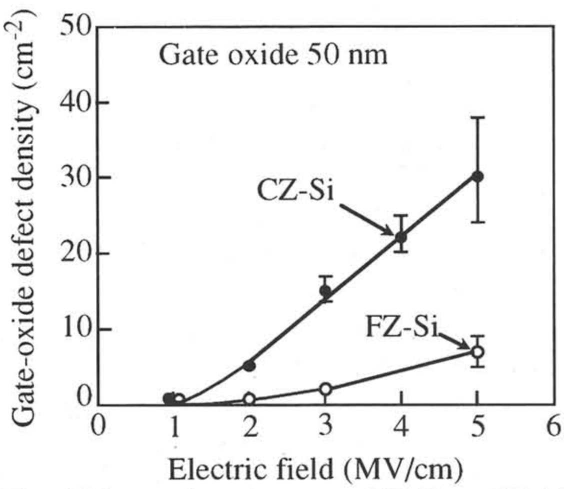

Fig. 1 Comparison between CZ-Si and FZ-Si.

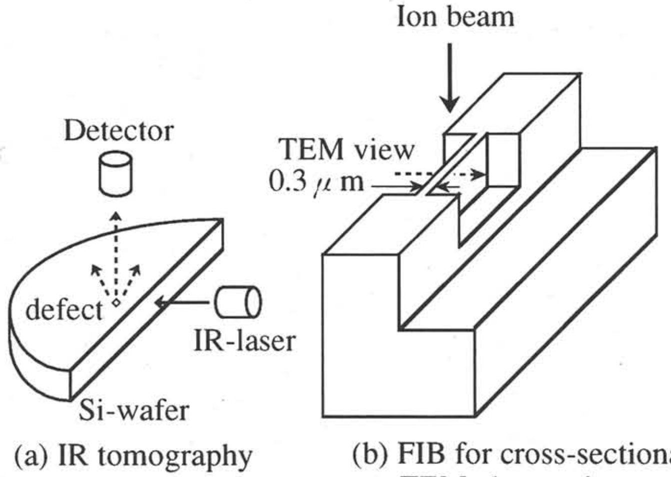

Fig. 2 A schematic illustration of specimen preparation.

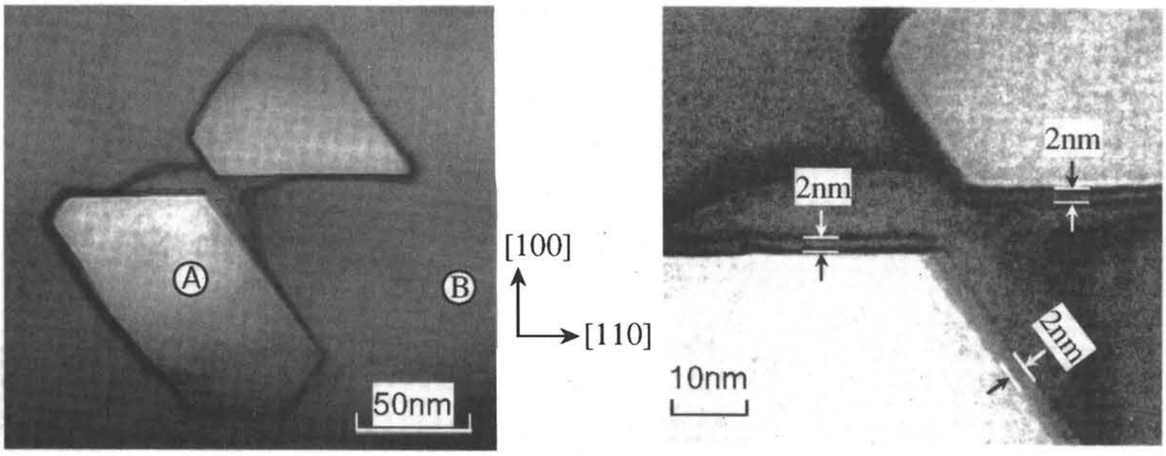

(a) Twin octahedron structure

(b) Side wall structure of the defect

Fig. 3 Cross-sectional TEM observation of grown-in defect.

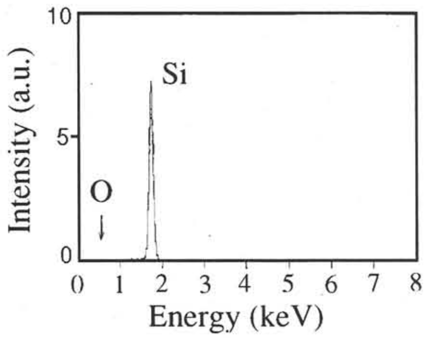

(a) Point A in Fig. 3(a)

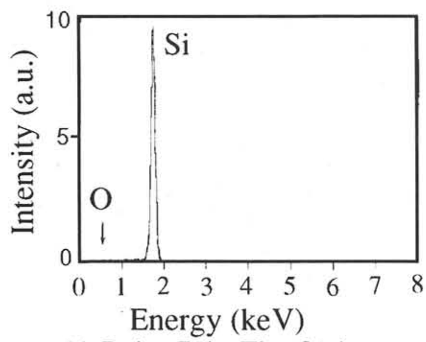

(b) Point B in Fig. 3(a)

Fig. 4 EDS spectra of the grown-in defect.

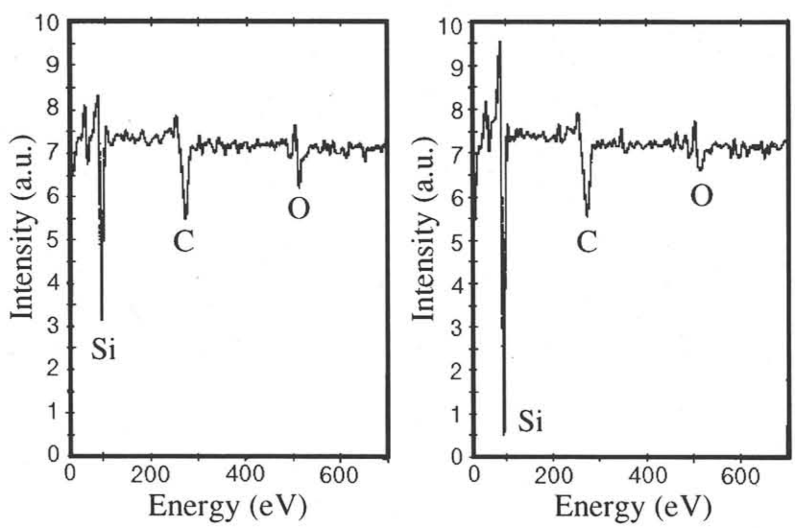

(a) Point A in Fig. 3(a)

(b) Point B in Fig. 3(a)

Fig. 5 AES spectra of the grown-in defect.